

Formulation of stability-dependent empirical relations for turbulent intensities from surface layer turbulence measurements for dispersion parameterization in a lagrangian particle dispersion model

K. B. R. Hari Prasad¹ · C. V. Srinivas¹ · A. N. V. Satyanarayana² · C. V. Naidu³ · R. Baskaran¹ · B. Venkatraman¹

Received: 5 July 2014 / Accepted: 17 February 2015 / Published online: 13 March 2015
© Springer-Verlag Wien 2015

Abstract Season- and stability-dependent turbulence intensity (σ_u/u_* , σ_v/u_* , σ_w/u_*) relationships are derived from experimental turbulence measurements following surface layer scaling and local stability at the tropical coastal site Kalpakkam, India for atmospheric dispersion parameterization. Turbulence wind components (u' , v' , w') measured with fast response UltraSonic Anemometers during an intense observation campaign for wind field modeling called Round Robin Exercise are used to formulate the flux–profile relationships using surface layer similarity theory and Fast Fourier Transform technique. The new relationships (modified Hanna scheme) are incorporated in a Lagrangian Particle Dispersion model FLEXPART-WRF and tested by conducting simulations for a field tracer dispersion experiment at Kalpakkam. Plume dispersion analysis of a ground level hypothetical release indicated that the new turbulent intensity formulations provide slightly higher diffusivity across the plume relative to the original Hanna scheme. The new formulations for σ_u , σ_v , σ_w are found to give better agreement with observed turbulent intensities during both stable and unstable conditions under various seasonal meteorological conditions. The simulated concentrations using the two

methods are compared with those obtained from a classical Gaussian model and the observed SF₆ concentration. It has been found that the new relationships provide comparatively higher diffusion across the plume relative to the model default Hanna scheme and provide downwind concentration results in better agreement with observations.

1 Introduction

Accurate representation of turbulent transport phenomena in atmospheric dispersion models is essential for better simulation of air pollution dispersion. The physical processes in atmospheric dispersion consist of transport and turbulent diffusion and deposition of air pollutants. Many scales of atmospheric motion such as micro, meso, and large-scale flows influence the Air pollution dispersion (Seaman 2000) and the characteristics of dispersion may vary across the scales depending on flow irregularities and mixing processes. Estimates from dispersion models typically depend on the treatment of horizontal and vertical turbulent diffusion and the meteorological data used in the calculation. Various models from simple box to complex fluid dynamics types based on different approaches such as Gaussian, Lagrangian/Eulerian have been used (Holmes and Morawska 2006) in the assessment of urban/industrial environmental pollution assessment. Lagrangian stochastic particle dispersion models (LPDM) are generally assumed to be more appropriate for simulating the atmospheric dispersion process as they track the particles moving by the action of winds and turbulence. In Lagrangian models, the displacement of fluid particles is treated by random motions (fluctuating velocities) and the particle evolution follows a Markov process. In these models, a Langevin

Responsible Editor: J.-F. Miao.

✉ C. V. Srinivas
venkatasrinivasc@yahoo.com; cvsri@igcar.gov.in

¹ Radiological Safety Division, RSEG, Indira Gandhi Centre for Atomic Research, Kalpakkam 603102, India

² Centre for Land–Ocean–Rivers and Atmospheres, Indian Institute of Technology, Kharagpur, India

³ Department of Meteorology and Oceanography, Andhra University, Visakhapatnam 530003, India

stochastic differential equation is used to describe the evolution of the particles, wherein the particle velocities are computed by the combination of a deterministic term and a stochastic one (Zannetti 1990). The fluid particle trajectory equation involves a transport term computed with mean wind and a turbulent diffusion term computed from velocity fluctuation. The turbulent velocity fluctuation or variances are parameterized using different methods (Wilson and Sawford 1996). The LPDMs use the time- and space-varying mean meteorological outputs from mesoscale atmospheric models to represent the inhomogeneity in the flow field over complex terrain such as coastal, urban and hilly regions. Due to the natural way of representation of turbulent transport in LPDMs, they are highly preferred to simulate the dispersion phenomena in special situations such as presence of complex topographies, low wind velocities and spatial and temporal variations of the meteorological fields (Carvalho et al. 2002). Various methods have been proposed for treatment of turbulent diffusion of pollutants in dispersion models based on availability of crucial parameters such as vertical temperature/wind profiles, turbulent kinetic energy (TKE), and turbulent fluxes. The efficiency of diffusion schemes depends on how well they can capture the extremities in mixing leading to realistic concentration estimates. The complex schemes involve more details of input parameters. In the random-walk dispersion model, SPEEDI turbulent diffusivity is estimated using Pasquill–Gifford (PG) stability categories (Imai et al. 1985). In the Lagrangian Puff model HYSPLIT (Draxler 1992), several alternative methods of diffusion estimation (Beljaars and Betts 1993; Deardorff 1973; Holtslag and Boville 1993; Kantha and Clayson 2000; Smagorinsky 1963; Troen and Mahrt 1986) are used. In the AERMOD dispersion model, the diffusion is assumed to be Gaussian/bi-Gaussian under stable/convective conditions (Willis and Deardorff 1981). The concentration estimates may vary according to the diffusion schemes which need evaluation for their application at any given region or location.

In many short-range diffusion schemes, the horizontal and vertical velocity variances are computed from the stability parameters calculated from flux–profile relationships. Hanna (1982) developed a parameterization for wind velocity fluctuations for application in dispersion models using planetary boundary layer (PBL) similarity theory. This parameterization was arrived based on analysis of experimental field data sets (Hanna 1968, 1982; Kaimal et al. 1976, 1982) and theoretical considerations (Irwin 1979; Panofsky et al. 1977). In Hanna's scheme, the turbulent wind fluctuations are parameterized in terms of PBL height, Monin–Obukhov length, roughness length, convective velocity scale, and friction velocity. Based on these boundary layer scaling parameters, the earlier workers

developed some universal relationships for different stability conditions i.e., Unstable, Stable and Neutral conditions. Stohl et al. (2005) incorporated the Hanna's parameterization in their FLEXPART LPDM. Hanna's scheme is a widely used parameterization in many dispersion models over a large number of terrain and topographic conditions and climate conditions. The empirical relationships for turbulent intensities (σ_u/u_* , σ_v/u_* , σ_w/u_*) are assumed valid without verification and adopted over different regions and weather conditions for the study of dispersion. Studies indicate the Hanna's formulations may not hold good universally (Moreira et al. 2011). Observational analysis would be required to verify the relations and to propose new formulations for application under seasonally varying atmospheric conditions. The present study aims to develop site-specific and season-dependent relationships for wind velocity fluctuations i.e., turbulent intensities (σ_u/u_* , σ_v/u_* , σ_w/u_*) based on normalized turbulent wind fluctuations and stability parameter (z/L) and implement the relationships in FLEXPART-WRF dispersion model by testing their performance against experimental dispersion data sets for application at the coastal site Kalpakkam.

2 Brief description of observation site and meteorological measurements

The study location Kalpakkam (12°30'N; 80°10'E) is situated in the southern India. It is a coastal site located about 70 km south of Chennai metropolitan city. The observation site has a plain terrain with elevation varying from 6 m above mean sea level (AMSL) at the coast to 20 m AMSL inland. The vegetation comprises mainly grass, dry and irrigated crop lands. The soil texture varies from silt loam at the coast to sandy clay loam inland. A multi-level 50-m micrometeorological tower equipped with slow and fast response sensors for measurement of wind, temperature and humidity observations is located at Anupuram township situated about 6 km away from the coast in Kalpakkam. The tower is installed on a plain grass land with a clear fetch of 300 m with no tall buildings and structures around. The surface around the tower is covered with mud and grass which grows up to a height of 20–50 cm during northeast monsoon season. The meteorological tower is equipped with slow response NRG-make sensors (cup anemometers, wind vanes, temperature and humidity sensors) to measure the wind speed, wind direction, temperature and humidity at different arbitrary levels (2, 8, 16, 32, and 50 m) and a fast response UltraSonic Anemometer at 10-m level to measure the turbulent fluxes. The Sonic Anemometer measures the fluctuating wind components along the three orthogonal co-ordinate directions N–S, E–

W and the vertical based on the transit time of ultrasonic acoustic signals. The fast response data acquired at 10 Hz frequency are used in the development of turbulent intensity relations in the present study. The winds at the observation site vary as southwesterly during southwest monsoon (June–September), northeasterly in winter monsoon (October–November), westerly during winter (December–February) and southerly during summer (March–May). The roughness parameter at the site varies as 10–15 cm due to all seasons with low wind conditions except the southwest monsoon in which the roughness parameter is about 7.5 cm due to strong winds.

3 Methodology

3.1 Description of dispersion model

In this study, the Lagrangian particle model FLEXPART-WRF (Stohl et al. 2005) is used to simulate the dispersion at the coastal site Kalpakkam. This model simulates the mesoscale transport, diffusion, dry and wet deposition, and radioactive decay of emissions released from point, line, area or volume sources by computing trajectories of fluid particles (Stohl et al. 2005). The model is widely used in radiological plume dispersion analysis and impact studies (Srinivas et al. 2012, 2014; among others). FLEXPART-WRF uses the time-varying 3D meteorological fields simulated by the mesoscale meteorological model WRF (Doran et al. 2008; Fast and Easter 2006). FLEXPART uses a zero acceleration scheme to compute the particle trajectories, in which particle movements are dependent on grid-scale winds and the turbulent fluctuations. The trajectory equation is written as

$$X(t + \Delta t) = X(t) + v(X, t)\Delta t \tag{1}$$

where ‘*t*’ is the time, ‘ Δt ’ the time increment, ‘*X*’ the position vector and ‘*v*’ is the wind velocity. The velocity ‘*v*’ is taken to be the sum of grid-scale mean wind (*v*), turbulent wind fluctuation (*v_t*) and mesoscale wind fluctuation (*v_m*) as given in Zannetti (1992). The turbulent velocity *v_t* is parameterized following Markov process using the Langevin equation (Thomson 1987) as

$$dv_{ti} = a_i(x, v_i, t)dt + b_{ij}(x, v_i, t)dW_j \tag{2}$$

where ‘*a*’ is the drift term, ‘*b*’ is the diffusion term, which are functions of position, turbulent velocity and time. *dW_j* are incremental components of a Wiener process with mean zero and variance ‘*dt*’, which are uncorrelated with other components and uncorrelated in time (Legg and Raupach 1982). The Langevin equation for the vertical wind component is given by

$$dw = -w \frac{dt}{\tau_{L_w}} + \frac{\partial \sigma_w^2}{\partial z} dt + \frac{\sigma_w^2}{\rho} \frac{\partial \rho}{\partial z} dt + \left(\frac{2}{\tau_{L_w}}\right)^{1/2} \sigma_w dW \tag{3}$$

where ‘*w*’ is the turbulent wind component, σ_w is the standard deviation of the turbulent vertical wind component, ‘ τ_{L_w} ’ is the Lagrangian time scale for the vertical velocity autocorrelation and ‘ ρ ’ is the density. The second and third terms on right hand side of Eq. (3) are the drift correction (McNider et al. 1998) and density correction (Stohl and Thomson 1999), respectively. To solve the above equation, data on $\sigma_{v_{ti}}$, and τ_{L_i} are required at any time and position of the particle trajectory. To represent the transport in the boundary layer more accurately, the time step in the FLEXPART is limited by the Lagrangian time scale τ_L , which is implicitly estimated using the relation.

$$\Delta t_i = \frac{1}{cfl} \min\left(\tau_{L_w}, \frac{h}{2w}, \frac{0.5\sigma_w}{\partial \sigma_w / \partial z}\right) \tag{4}$$

Since the vertical wind component is the most important one, only τ_{L_w} is used for the determination of time step. This computed Δt_i is used to solve the Langevin equations for the horizontal turbulent wind components. The minimum value of Δt_i used is one second. For solving the Langevin equation for the vertical wind component, a shorter time step $\Delta t_w = \Delta t_i / \text{ifine}$ is used. The Langevin equation requires turbulence intensities ($\sigma_{v_{ti}}$) and Lagrangian time scale (τ_{L_i}). Hanna (1982) proposed a scheme for determination of $\sigma_{v_{ti}}$ and τ_{L_i} based on boundary layer parameters mixed layer height (*h*), Monin–Obukhov length (*L*), convective velocity scale (*w_{*}*), roughness length (*z_o*) and friction velocity (*u_{*}*). The Hanna parameterization is presently used in FLEXPART for obtaining the wind fluctuations. The relationships for Lagrangian time scales (τ_{L_i}) in terms of intensity of turbulence σ_i , given by Hanna (1982) for various stability conditions are provided below.

Unstable conditions:

$$\frac{\sigma_u}{u_*} = \frac{\sigma_v}{u_*} = \left(12 + \frac{h}{2|L|}\right)^{1/3} \tag{5}$$

$$\frac{\sigma_w}{u_*} = \left[1.2w_*^2 \left(1 - 0.9 \frac{z}{h}\right) \left(\frac{z}{h}\right)^{2/3} + \left(1.8 - 1.4 \frac{z}{h}\right) u_*^2\right]^{1/2} \tag{6}$$

$$T_{Lu} = T_{Lv} = 0.15 \frac{h}{\sigma_u} \tag{7}$$

$$T_{Lw} = 0.1 \frac{z}{\sigma_w [0.55 - 0.38(z - z_0)/L]} \tag{8}$$

Neutral conditions:

$$\frac{\sigma_u}{u_*} = 2.0 \exp(-3fz/u_*) \tag{9}$$

$$\frac{\sigma_v}{u_*} = \frac{\sigma_w}{u_*} = 1.30 \exp(-2fz/u_*) \quad (10)$$

$$T_{Lu} = T_{Lv} = T_{Lw} = \frac{0.5z/\sigma_w}{1 + 15fz/u_*} \quad (11)$$

Stable conditions:

$$\frac{\sigma_u}{u_*} = 2.0 \left(1 - \frac{z}{L}\right) \quad (12)$$

$$\frac{\sigma_v}{u_*} = \frac{\sigma_w}{u_*} = 1.3 \left(1 - \frac{z}{L}\right) \quad (13)$$

$$T_{Lu} = 0.15 \frac{h}{\sigma_u} \left(\frac{z}{h}\right)^{0.5} \quad (14)$$

$$T_{Lv} = 0.07 \frac{h}{\sigma_v} \left(\frac{z}{h}\right)^{0.5} \quad (15)$$

$$T_{Lw} = 0.1 \frac{h}{\sigma_w} \left(\frac{z}{h}\right)^{0.5} \quad (16)$$

The boundary layer parameters (h , L , w_* , z_0 , u_*) required in the above formulations are taken from the mesoscale model WRF outputs for dispersion simulation.

3.2 Derivation of new relationships for turbulent intensities

In the present work, new relations for turbulent intensities (hereafter called modified Hanna relationships) are derived from turbulence measurements following Monin–Obukhov (M–O) similarity theory. The observational data generated under Round Robin Exercise (RRE-2010) (Srinivas et al. 2011) project aiming to validate various models over Kalpakkam in different spatial scales are used to develop season-dependent relationships based on normalized turbulent wind fluctuations (σ_i/u_* ; where $i = u, v, w$) and stability parameter (z/L).

The analysis is done using the data measured by a fast response Ultra Sonic Anemometer mounted at 10-m level on the meteorological tower. The Sonic Anemometer is a fast response sensor and records all the 3D wind components and virtual temperature at 10 Hz and stores in a Campbell data logger. According to Monin–Obukhov Similarity Theory (MOST) (Businger et al. 1971; Dyer 1974; Stull 1988), when the turbulent fluctuations are normalized by surface layer scaling parameters (i.e., σ_i/u_*), we can obtain universal relationships with respect to the non-dimensional stability parameter (z/L), where z is the height of measurement and L is the Monin–Obukhov length. Observation analysis following MOST provides site-specific relationships. McBean (1971) found that these relationships depend on the spatial and temporal inhomogeneities of the atmospheric motions and they are also dependent on the atmospheric stability. Many investigators suggest that, only modeling coefficients in

these relationships vary as per site topography and regional atmospheric conditions. Singha and Sadr (2012) reported that the modeling coefficients are function of climatic conditions, geographical location of the measuring site, dynamic and the thermal characteristics of the atmosphere. So these relationships are site specific and season dependent. Before performing the analysis, first the data sets are subjected to extensive quality checks. The technique proposed by Vickers and Mahrt (1996) is adopted to remove spikes in the data. Using this method, mean and standard deviation (SD) are computed for a series of moving windows of length 5 min and the window moves one point at a time through the series. Any data point that is more than 3.5 SD from the window mean is considered as spike and is replaced with value obtained by linear interpolation between data points. The method proposed by Wilcjack et al. (2001) is used to place the sonic coordinates in mean stream direction for tilt correction and double rotation. Linear detrending is used to separate the eddy fluxes from the slowly varying atmospheric motions. Data sets are subjected to spectral analysis and those falling in Kolmogorov $-5/3$ inertial subrange are retained and the data sets that do not satisfy the universal relationship are rejected.

Fast Fourier Transformation method is used to calculate the energy spectrum of the 3D wind components. Fourier transformation converts the time domain into frequency domain (Kaimal et al. 1972). Eddy covariance method separates the instantaneous signal into the mean and fluctuating parts (Metzger and Holmes 2008; Vecenaj et al. 2011, 2012). Using Reynolds averaging method, we can define the mean, variance, covariance and we can simplify the equations of turbulent flow (Stull 1988). Based on the assumption of spectral gap presented in horizontal wind speed spectrum, we separated the instantaneous components into mean and fluctuating parts. This spectral gap separates the large-scale motions from the microscale eddies. The present grid point models use spatial resolutions in this spectral gap regions, implying that they can resolve large-scale motions but sub-grid scale features have to be parameterized. Using Reynolds averaging technique, non-stationary atmospheric motions are transformed into statistically stationary time series (Karmen et al. 2012). Even though turbulent motions are non-stationary, turbulent flows are statistically stationary (Karmen et al. 2012). This statistically stationary approach is achieved using the mean removal or filter. Normally 10–60-min time period is taken as the averaging time interval (Onclay et al. 1996). For the present study, 30-min time period is taken as the averaging period to compute the standard deviation of velocity components.

From similarity theory, various scaling parameters can be defined.

$$\text{Length scale } L = \frac{-u_*^3 T}{gk w' T'} \tag{17}$$

$$\text{Velocity scale } u_* = \left(\overline{u'w'^2} + \overline{v'w'^2} \right)^{1/4} \tag{18}$$

where the prime quantities represent the turbulent fluctuations from the mean. Using these scaling parameters, the dimensionless standard deviation of the wind components (σ_u/u_* , σ_v/u_* , σ_w/u_*) can be obtained. According to MOST, normalized turbulent components of wind (σ_u/u_* , σ_v/u_* and σ_w/u_*) are universal functions of the stability parameter (z/L) i.e.,

$$\frac{\sigma_i}{u_*} = A_i \left[1 + B_i \left| \frac{z}{L} \right| \right]^{C_i} \tag{19}$$

where $i = u, v, w$ and A_i, B_i and C_i are the site-specific modeling coefficients. Three stability categories were identified based on the stability parameter z/L (Golder 1972) as given below

$-0.09 < z/L < 0.09$ near neutral

$z/L > 0.09$ stable

$z/L < -0.09$ unstable

In the near neutral range ($-0.09 < z/L < 0.09$), the turbulence is assumed to be isotropic and default Hanna relations are assumed valid. Hence, the relationships are developed for the stable and unstable categories alone based on observation analysis in each season. For neutral conditions, the default Hanna relations are followed. The data are analyzed seasonally considering a total of 10 days period in each season i.e., winter (1–10 January 2011), summer (20–30 April 2011), southwest monsoon (1–15 September 2010) and post-monsoon (20–30 October 2010). Though a window of 10-day period alone in each season is considered for analysis, it is designed in such a way that it falls in the middle of each season, represents major seasonal features, covers fair weather conditions required for the analysis as well as avoids gaps in observations. The dispersion parameters in the dispersion model can be parameterized in terms of the derived turbulent intensities to estimate the concentrations and for validation with the observed concentrations.

3.3 Dispersion data

Measured concentrations from a field tracer dispersion experiment are used to test the new relationships of turbulent intensities in FLEXPART for the site region. The tracer experiment at Kalpakkam was conducted on a plain terrain under a southeasterly flow characterized with a slightly unstable atmosphere on 12 April 2013 (Srinivas et al. 2013) in a short range of 500 m. During the

experiment, SF₆ gas was released at 1 m above ground level (AGL) using a mass flow controller at a flow rate of 2 lpm (~0.22 g/s) from 8.30 to 9.00 IST.

3.4 Numerical simulations

The derived turbulent intensities are incorporated in the Lagrangian Particle Dispersion model (LPDM) FLEXPART-WRF. Two cases of dispersion simulations are conducted to test the new relationships. The first case consists of four sets of simulations of hypothetical release in four different seasonal conditions over the Kalpakkam site. This helps to analyze the differences in the spatial plume simulated up to few tens of kilometers with the two relationships for turbulent intensities under various seasonal conditions at the site. The second case consists of simulation for a Tracer Release experiment at Kalpakkam. In all the cases, the input meteorological fields are simulated with Advanced Research Weather Research and Forecast model (ARW).

The ARW model is configured with 4 nested domains (Fig. 1) with resolutions of 27, 9, 3, 1 km and the inner most nest covering the study domain with 190 × 190 grids. A total of 50 vertical levels are used in all cases. The WRF model was evaluated for the study region in the previous studies (Hari prasad et al. 2014) for the simulation of near-surface winds, temperature, humidity and planetary boundary layer (PBL) structure with different PBL schemes. It has been found that the model well simulated various parameters with the Hong et al. (2006) Yonsei University non-local scheme. Hence, in this study, the YSU

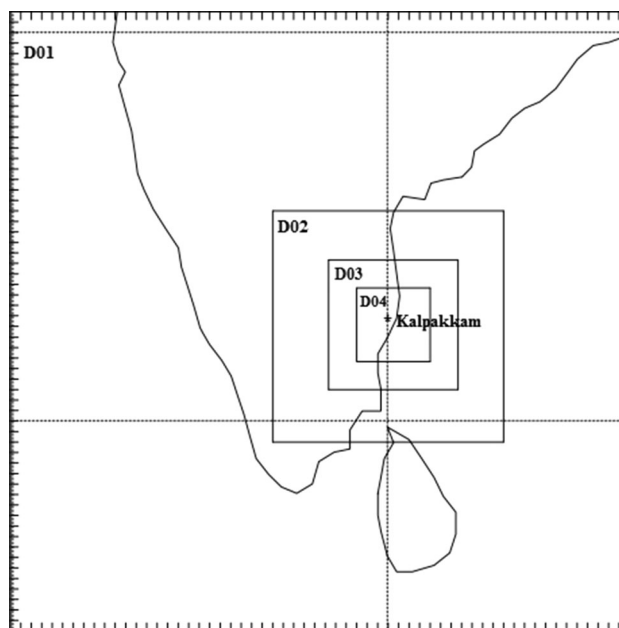


Fig. 1 Domains used in ARW model for Kalpakkam, India

scheme is adopted. Second, an option in YSU PBL for representing the topographic effects on surface winds (Jimenez and Dudhia 2012) as a function of topographic height and standard deviation of sub-grid scale orography is used to obtain realistic simulation of near-surface meteorological variables. The other physics options used in simulations are Kain–Fritsch for convection, RRTM for longwave, Dudhia scheme for shortwave, Noah land surface model, MM5 surface layer similarity theory. The National Centre for Environmental Prediction (NCEP) Global Forecast System (GFS) 50 km resolution meteorological analysis and 3 hourly forecasts are used for initial and boundary conditions. For the first case, four simulations are conducted with ARW and the model is initialized at 00 UTC on 14 January, 12 April, 22 September and 2 October 2010 and integrated for 48 h in each case. For the second case (Kalpakkam dispersion experiment), ARW is initialized at 00 UTC on 12 April 2013 and integrated for 24 h.

In all dispersion simulations, the FLEXPART is configured with 200×200 horizontal grids each of 100 m resolution, 11 vertical levels from the surface up to 2000 m height above ground level (AGL) with the lowest level between 0 and 25 m AGL. A total of 300,000 pseudoparticles were released in the simulation. In FLEXPART, a constant time step can be defined in terms of synchronization interval of all processes and this time step is typically a few hundred seconds. The use of such fast time step leads to low autocorrelations between turbulent velocity fluctuations, under representation of turbulence in the boundary layer and underestimation of surface concentrations. Hence, in the present work to ensure a more realistic simulation of PBL transport and concentrations, the time step is implicitly estimated using Eq. (4) with controlling parameters ‘CTL’ (limiting factor of time step for horizontal turbulent winds) and ‘ifine’ (limiting factor of time step for vertical turbulent winds) defined as 5 and 4, respectively. The minimum time step used in the model is 1 s. In all cases, simulations are conducted using default Hanna diffusion scheme as well with modified Hanna parameterization scheme. Concentrations are sampled at every 60 s and averaged over 1800 s and outputs are drawn at every 3600 s. For the first case, four simulations covering 14–16 January 11 (winter), 12–14 April 11 (summer), 22–24 September 10 (monsoon) and 2–4 October 10 (post-monsoon) are conducted assuming a hypothetical ground level continuous point source (SF_6) of 1 g/s emission rate located near the coast (12.5584°N , 80.1700°E). For this case model, simulated turbulent intensities with default Hanna parameterization and the new scheme are compared with observed turbulent intensities derived from sonic anemometer data at observation location Kalpakkam. For the second case (SF_6 tracer experiment at Kalpakkam),

simulation with FLEXPART is conducted for a 24-h period on 12 April 2013 with a release of 0.22 g/s and the simulated SF_6 mixing ratios obtained using default Hanna and new relationships are compared against measured mixing ratios.

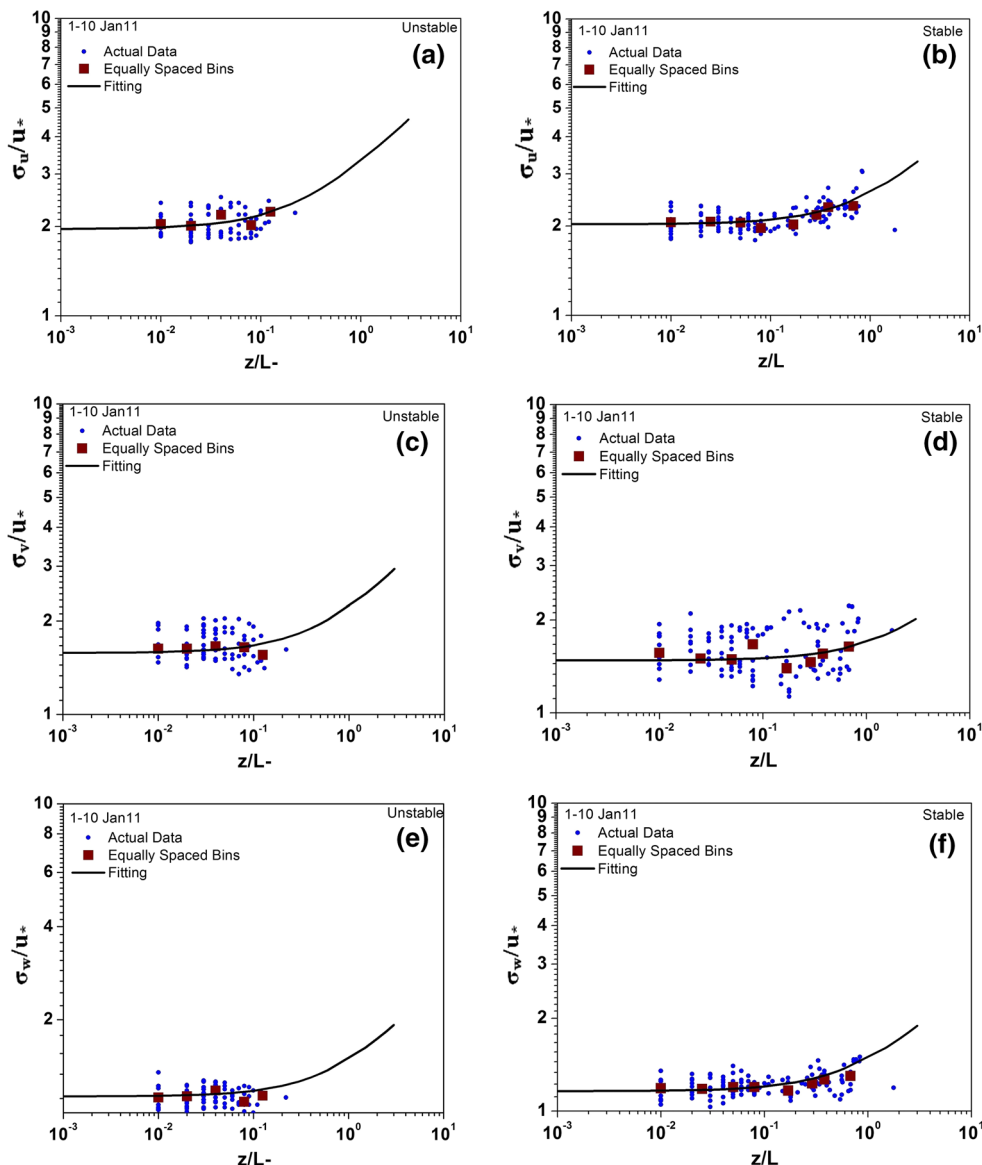
4 Results

The results of stability-dependent turbulent intensity relations for various seasons derived using M–O theory are presented in Sect. 4.1. Further, the results of dispersion analysis from FLEXPART using the default Hanna scheme and modified Hanna formulations are discussed in Sect. 4.2. Subsequently measured air concentration data obtained from dispersion experiment are used to test the new turbulent intensity formulations along with statistical analysis.

4.1 Turbulent intensity relationships

The variation of normalized intensity of turbulence (Dimensionless standard deviation of wind components) with stability parameter (z/L) is shown in Figs. 2, 3, 4, and 5 for different seasons. It is noted that the clustering of the data points with stability factor (z/L) is unique in each case. This shows the variation in turbulence characteristics in different seasons. In this plot, continuous line represents the mean of the scattered data. In all cases, the turbulence intensity, in general, is noted to increase with z/L i.e., increase in instability. Second, the increasing characteristic of turbulence intensity is uniquely represented in each of the momentum components (zonal, meridional and vertical velocity distributions). The intensities are closely clustered in January (winter), widely separated in summer (April) and monsoon (September) and in post-monsoon (October). The close scatter of turbulence intensities in winter could be due to production of turbulence mainly by shear in both day and night times and with similar order of turbulence. The large scatter of turbulence intensities during summer and monsoon seasons could be due to large convective turbulence (buoyancy) in the daytime in comparison to mechanical (shear) turbulence in the night time. In all the seasons, the intensities are closely clustered during stable conditions indicating relatively uniform intensity with stable stratification. It is seen that the magnitudes of the intensities are varying between different seasons. In September (SW monsoon), the growth of (σ_w/u_*) is more relative to other months. This type of increasing normalized turbulence intensity with instability is more evident in September, October, April months. But in January, this type of pattern is not seen due to relatively stable atmospheric stratification. From these plots, we see that the

Fig. 2 Variation of normalized intensity of turbulence of zonal (u), meridional (v) and vertical (w) winds at Kalpakkam during unstable and stable atmospheric conditions in winter season. *Left panels (a, c, e)* are for unstable and *right panels (b, d, f)* are for stable conditions. *Top (a, b), middle (c, d) and bottom (e, f) panels* are for normalized standard deviations for u , v , w components, respectively



variation of turbulence intensity with z/L changes from season to season. Using trend lines, relationships of turbulent intensity with stability are developed for different seasons and presented in Table 1. We see that the functional relationships of turbulence intensity with z/L widely varied with respect to two broad stability types (stable, unstable) as well as with respect to seasons.

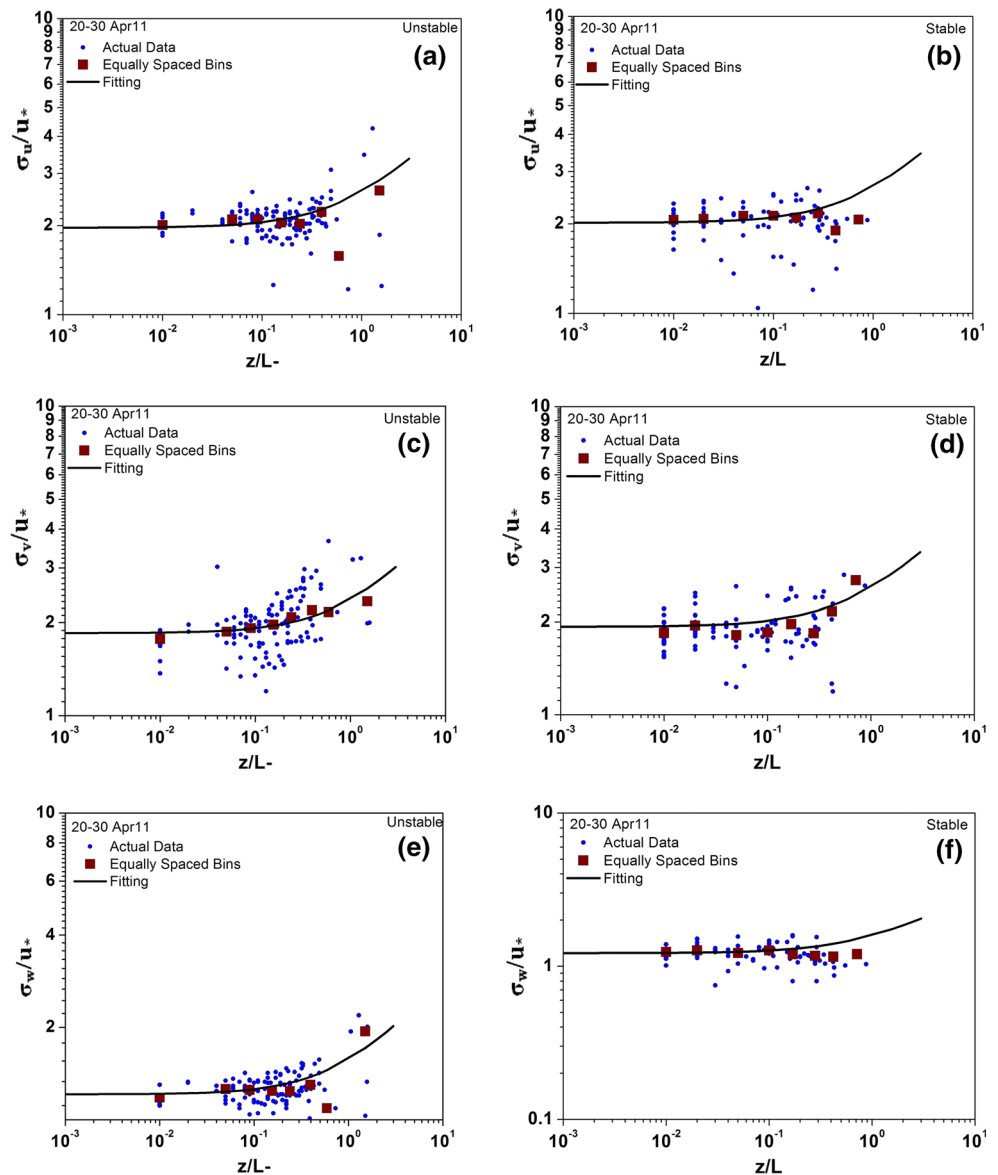
4.2 Plume dispersion analysis in the four seasons

In an attempt to study the variation in the atmospheric dispersion arising from the use of site-specific turbulent intensity relationships, we examined the results of dispersion simulations made using default Hanna scheme and the new formulations for few days in different seasons. The meteorological condition at the site varied with seasons

with large-scale flow as northeasterly during winter, westerly during summer, southwesterly during monsoon and southerly during the post-monsoon. The land–sea breeze is the predominant local-scale flow at the site. The temporal plume trajectory varied on each day according to the prevailing large-scale flow pattern and the diurnal local circulations at the site in these seasons. The plume concentration distribution for a unit release of a tracer pollutant (SF_6) is presented from the simulations with the default Hanna’s scheme and the newly arrived (modified) Hanna scheme for the representative days of each season.

Simulated plume ground level (0–25 m AGL) concentration distribution for the stable and unstable atmospheric conditions is presented on 14 Jan 2011 in Fig. 6 for the winter season. This shows the concentration per unit release (also called the dilution factor) at every point in the

Fig. 3 Variation of normalized intensity of turbulence of zonal (u), meridional (v) and vertical (w) winds at Kalpakkam during unstable and stable atmospheric conditions in summer season. *Left panels (a, c, e)* are for unstable and *right panels (b, d, f)* are for stable conditions. *Top (a, b), middle (c, d) and bottom (e, f) panels* are for normalized standard deviations for u , v , w components, respectively

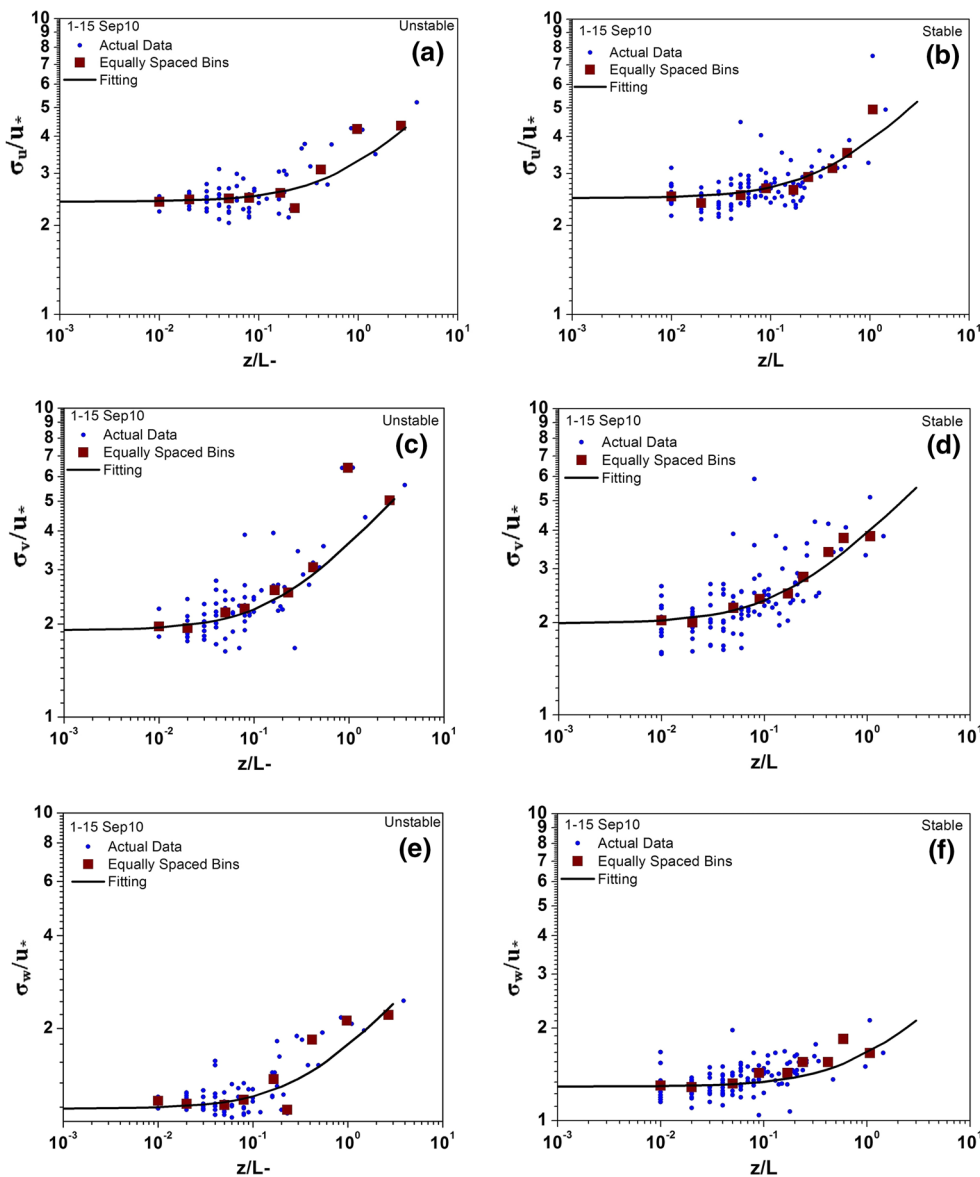


plume. For the winter flow condition, the simulated plume is oriented to south–southwest in the morning stable atmosphere and to the southwest in the daytime unstable atmosphere. While the plume trajectories are not different in the two simulations, differences are noted in the concentration distribution especially during unstable condition. In both the above conditions, relatively wider plume and higher concentration are found along plume centerline with modified Hanna scheme. The wider plume simulated in the case of modified Hanna scheme is evident from relatively larger cross-wind dispersion. To study this aspect, the Gaussian concentration plots across the plume for the downwind distances of 1, 3, 5, and 7 km from the source are analyzed (not shown) for unstable condition as an example. Here, the stabilities are determined from the non-dimensional stability parameter (z/L) obtained from WRF

simulations as per Golder (1972) method. It has been found that as the distance from the source increases, a clear difference in concentration between the two simulations is apparent. The normal concentration distribution plots indicate slightly larger standard deviation with modified Hanna scheme after 3 km than the Hanna scheme indicating relatively higher diffusion with modified Hanna scheme.

The changes in diffusivities using the two formulations for turbulent intensities are analyzed from the time variation in turbulent intensities in the zonal, meridional and vertical directions (σ_u , σ_v , σ_w) from simulations with each of the schemes (Hanna, modified Hanna) and comparison with corresponding values derived from turbulence observations at observation location Kalpakkam (Fig. 7). The observed turbulent intensities are derived from fluctuating

Fig. 4 Variation of normalized intensity of turbulence of zonal (u), meridional (v) and vertical (w) winds at Kalpakkam during unstable and stable atmospheric conditions in monsoon season. *Left panels (a, c, e)* are for unstable and *right panels (b, d, f)* are for stable conditions. *Top (a, b), middle (c, d) and bottom (e, f) panels* are for normalized standard deviations for u , v , w components, respectively



wind components (u' , v' , w') measured by a fast response Sonic Anemometer at Kalpakkam station as mentioned in Sect. 3.2. We find that there are large differences in the simulated turbulent intensities (σ_u , σ_v , σ_w) from both the simulations especially during daytime unstable conditions (0400 UTC–1200 UTC) and the differences minimize in the neutral/stable night conditions. During unstable daytime condition, it is noted that modified Hanna scheme provides a better comparison of turbulent intensities with observed turbulent intensities compared to those obtained with default Hanna scheme. During the stable condition, both the schemes (Hanna, revised Hanna) yield similar and lesser turbulent intensities than the observed values.

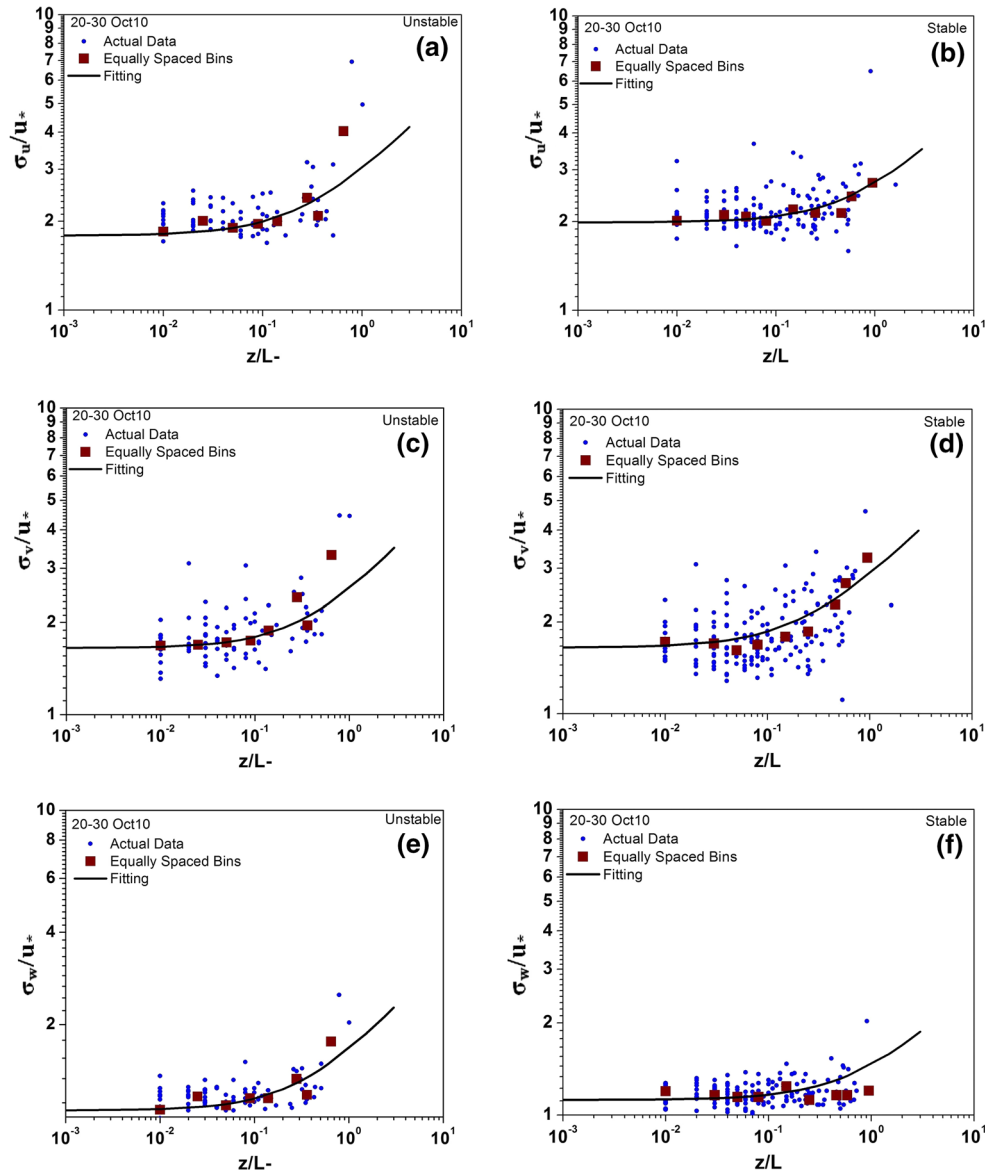
Similar results of relatively wider plume with modified Hanna scheme compared to the default Hanna scheme

are noted in the summer, monsoon and post-monsoon cases. The wider dispersion of the plume with modified Hanna scheme is more pronounced in the unstable condition in all these cases (not shown). Similar to the winter case, the daily cycle of simulated turbulent intensities in these cases indicated that the revised Hanna scheme gives more closer turbulent intensities to the observational estimates.

4.3 Comparison with measured concentration data

Hanna relationships for turbulent intensities are considered as Universal relationships. The reliability of the new formulations derived in the present study is tested using the measured concentration data from a tracer dispersion

Fig. 5 Variation of normalized intensity of turbulence of zonal (u), meridional (v) and vertical (w) winds at Kalpakkam during unstable and stable atmospheric conditions in post-monsoon season. *Left panels (a, c, e)* are for unstable and *right panels (b, d, f)* are for stable conditions. *Top (a, b), middle (c, d)* and *bottom (e, f) panels* are for normalized standard deviations for u , v , w components, respectively



experiment conducted at Kalpakkam coastal site on 12 April 2013. This experiment was conducted in a short distance range with a ground level release of SF₆ tracer gas in permissible limited quantities (Srinivas et al. 2013). Because of small quantities of release, the sampling of the concentrations is confined to a short distance up to 500 m from the release point to obtain detectable concentrations using the Gas Chromatograph. The measured mixing ratios of SF₆ tracer at 16 receptor points distributed between 25 and 500 m distance range in four sectors (100, 200, 300, and 400 m arcs) are used for the dispersion model comparison. To evaluate the dispersion model, statistical analysis is performed using error metrics of Correlation, root mean square error (RMSE), Fractional Variance (FS) and Fractional Bias (FB) as defined in Hanna (1989):

$$RMSE = \sqrt{\left(\frac{\sum_{i=1}^n (C_p - C_o)^2}{N}\right)} \tag{20}$$

$$FB = \frac{\overline{(C_o - C_p)}}{0.5(C_o + C_p)} \tag{21}$$

$$R = \frac{\overline{(C_o - \overline{C_o})(C_p - \overline{C_p})}}{\sigma_o \sigma_p} \tag{22}$$

$$FS = 2(\sigma_o - \sigma_p) / (\sigma_o + \sigma_p) \tag{23}$$

where N is total no. of samples, C_o is the observed concentration, C_p is the predicted concentration, σ_o , σ_p are the standard deviations of observation and predicted concentration, respectively, and the overbars represent the average of the variables.

Table 1 New relations between normalized intensity of turbulence to atmospheric stability in different seasons for Kalpakkam station

1–10 January 2011	21–30 April 2011	1–15 September 2010	20–30 October 2010
Unstable conditions			
$\frac{\sigma_u}{u_*} = 1.83 \left(1 - 4.98 \frac{z}{L}\right)^{1/3}$	$\frac{\sigma_u}{u_*} = 1.77 \left(1 - 3.36 \frac{z}{L}\right)^{1/3}$	$\frac{\sigma_u}{u_*} = 2.52 \left(1 - 2.02 \frac{z}{L}\right)^{1/3}$	$\frac{\sigma_u}{u_*} = 1.72 \left(1 - 5.18 \frac{z}{L}\right)^{1/3}$
$\frac{\sigma_v}{u_*} = 1.92 \left(1 - 9.56 \frac{z}{L}\right)^{1/3}$	$\frac{\sigma_v}{u_*} = 1.69 \left(1 - 3.91 \frac{z}{L}\right)^{1/3}$	$\frac{\sigma_v}{u_*} = 1.92 \left(1 - 9.8 \frac{z}{L}\right)^{1/3}$	$\frac{\sigma_v}{u_*} = 1.81 \left(1 - 1.6 \frac{z}{L}\right)^{1/3}$
$\frac{\sigma_w}{u_*} = 1.07 \left(1 - 1.21 \frac{z}{L}\right)^{1/3}$	$\frac{\sigma_w}{u_*} = 1.16 \left(1 - 1.21 \frac{z}{L}\right)^{1/3}$	$\frac{\sigma_w}{u_*} = 1.15 \left(1 - 3.55 \frac{z}{L}\right)^{1/3}$	$\frac{\sigma_w}{u_*} = 1.1 \left(1 - 1.91 \frac{z}{L}\right)^{1/3}$
Stable conditions			
$\frac{\sigma_u}{u_*} = 2.01 \left(1 + 1.21 \frac{z}{L}\right)^{1/3}$	$\frac{\sigma_u}{u_*} = 2.11 \left(1 + 0.31 \frac{z}{L}\right)^{1/3}$	$\frac{\sigma_u}{u_*} = 2.24 \left(1 + 6.98 \frac{z}{L}\right)^{1/3}$	$\frac{\sigma_u}{u_*} = 1.86 \left(1 + 3.18 \frac{z}{L}\right)^{1/3}$
$\frac{\sigma_v}{u_*} = 1.51 \left(1 + 0.65 \frac{z}{L}\right)^{1/3}$	$\frac{\sigma_v}{u_*} = 1.74 \left(1 + 1.81 \frac{z}{L}\right)^{1/3}$	$\frac{\sigma_v}{u_*} = 2.105 \left(1 + 8.6 \frac{z}{L}\right)^{1/3}$	$\frac{\sigma_v}{u_*} = 1.57 \left(1 + 4.4 \frac{z}{L}\right)^{1/3}$
$\frac{\sigma_w}{u_*} = 1.17 \left(1 + 0.65 \frac{z}{L}\right)^{1/3}$	$\frac{\sigma_w}{u_*} = 1.3 \left(1 + 1.01 \frac{z}{L}\right)^{1/3}$	$\frac{\sigma_w}{u_*} = 1.37 \left(1 + 1.04 \frac{z}{L}\right)^{1/3}$	$\frac{\sigma_w}{u_*} = 1.1 \left(1 + 1.11 \frac{z}{L}\right)^{1/3}$

The scatter plot for model predicted concentrations versus observed concentrations is presented in Fig. 8. It is seen that the predicted concentrations using modified Hanna scheme are in better agreement with the observed concentrations with higher correlation and lesser standard deviations as compared to the default Hanna scheme.

The concentration distribution at different arc distances 25, 50, 100, 200 m (Fig. 9) shows that the modified Hanna turbulent intensity relationships provide lesser concentration (i.e., larger dispersion) than the default Hanna scheme. The differences between the two schemes are noted to gradually increase away from the source point. Intercomparison of measured and simulated SF₆ mixing ratio shows that at all distances along the plume centerline, the new relationships provide lesser concentration indicating higher diffusivity in comparison to the Hanna scheme. Across the plume at all the distances, the new relationships (modified Hanna scheme) provide lesser concentrations indicating higher diffusivity relative to the model default Hanna scheme. Modified Hanna scheme has given more horizontal spread than the default Hanna scheme and it is comparable to the observed cross-wind horizontal spread with higher correlations, lesser fractional bias and lesser rmse relative to Hanna scheme (Table 2).

The simulated plume centerline concentrations using Hanna and modified Hanna schemes at different downwind distances (25, 50, 100, 200, 300, 400, 500, 600, 700, 800, 900 and 1000 m) are compared with measured concentrations and estimated values using classical Gaussian Plume dispersion model (GPM) and using same release and meteorological data inputs (wind speed, stability) as in FLEXPART (Fig. 10). While simulated centerline concentration with both Hanna and modified Hanna schemes of FLEXPART shows reasonable

agreement with measured data, GPM indicates higher concentrations up to a downwind distance of 250 m. Up to 200 m distance, both Hanna and modified Hanna scheme produced slightly higher concentrations relative to measurements. Appreciable differences in concentrations from Hanna and modified Hanna scheme are noticed below 100 m (near source) and above 500 m (away from source). The concentrations generated with modified Hanna scheme follow closely those obtained from GPM after 600 m distance.

5 Conclusions

Atmospheric turbulence data from a fast response Sonic Anemometer are analyzed for four seasons at the tropical coastal site Kalpakkam. Stability-dependent turbulent intensity relationships are derived from the turbulence measurements. The use of the new relationships for turbulent intensity (modified Hanna scheme) indicated wide differences in the diffusion parameterization among the four seasons. The semi-empirical formulations during summer and monsoon seasons produced relatively large turbulent intensities relative to the winter and post-monsoon conditions. The new relationships for turbulent intensity are incorporated in FLEXPART- WRF dispersion model and are tested for the four seasonal cases. An intercomparison of simulated turbulent intensities σ_u , σ_v , σ_w with FLEXPART with observed turbulence data (derived using Sonic Anemometer data) indicated the new relationships called the ‘modified Hanna’ provided better comparisons. It is found that the default Hanna scheme provides lesser turbulent intensities than observational estimates for all the three components σ_u , σ_v , σ_w . The higher diffusion with new

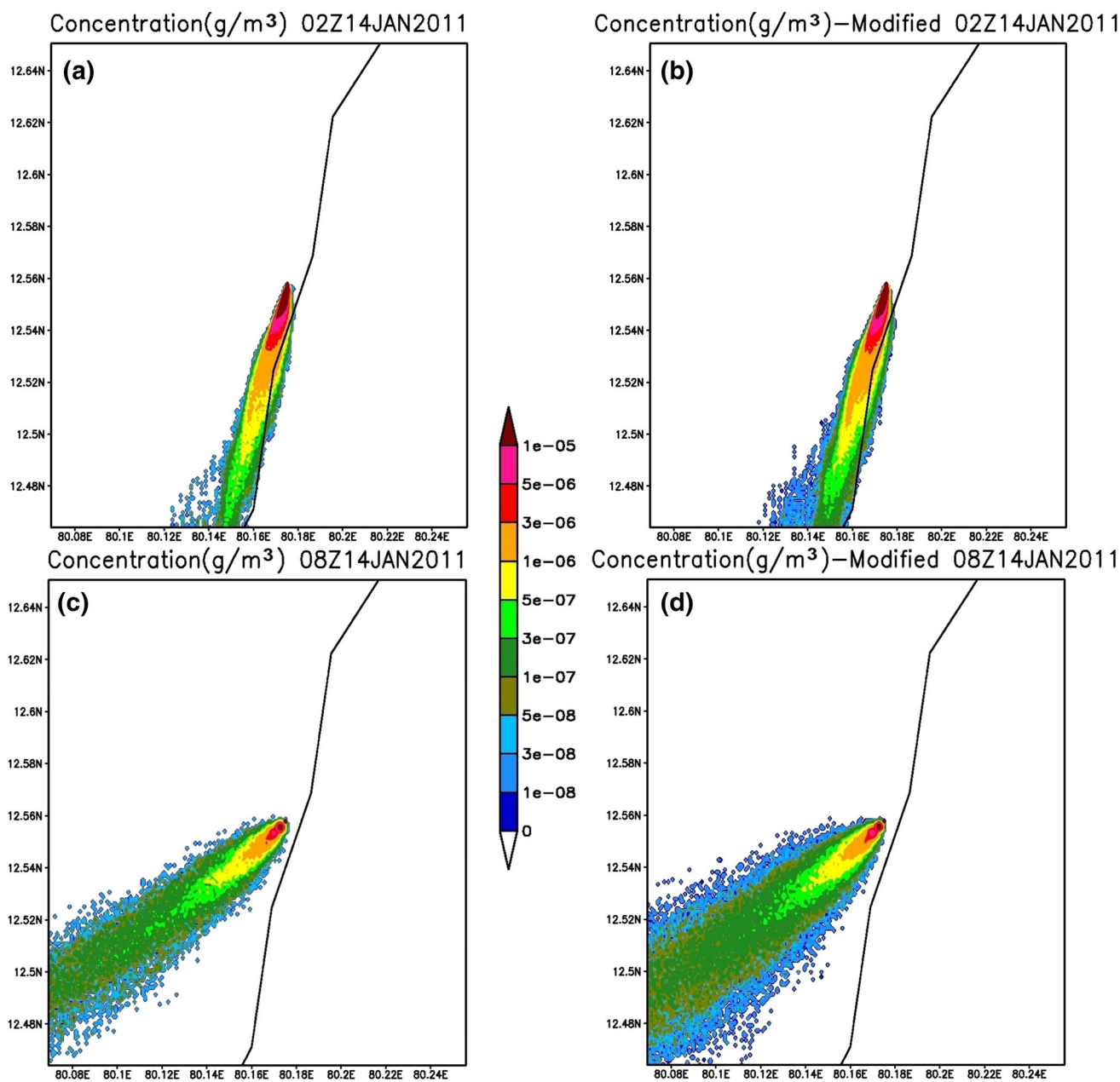


Fig. 6 Simulated plume dilution factor (g/m^3) for the winter case on 14 Jan 2011. The *top panels* (a, b) are for stable atmospheric conditions and *bottom panels* (c, d) are for unstable conditions. *Left*

panels (a, c) are for model default Hanna's diffusivities and *right panels* (b, d) are for modified Hanna's relationships

scheme is also noticed in the simulated plume concentration pattern of the four seasonal cases. To confirm the above results, data obtained from a field tracer dispersion experiment held on 12 April 2013 during a southeasterly flow condition at the Kalpakkam coastal site are used for comparisons. Simulations with the Hanna scheme and the modified Hanna scheme and their comparisons with actual

concentrations obtained from the experiment clearly indicated that the modified Hanna scheme gives lesser concentrations than the model default Hanna scheme. Statistical analysis of the simulated concentrations with observations clearly shows that the modified Hanna scheme produces better comparisons with the observations in terms of reduction in RMSE, Fractional Bias, Fractional Variance

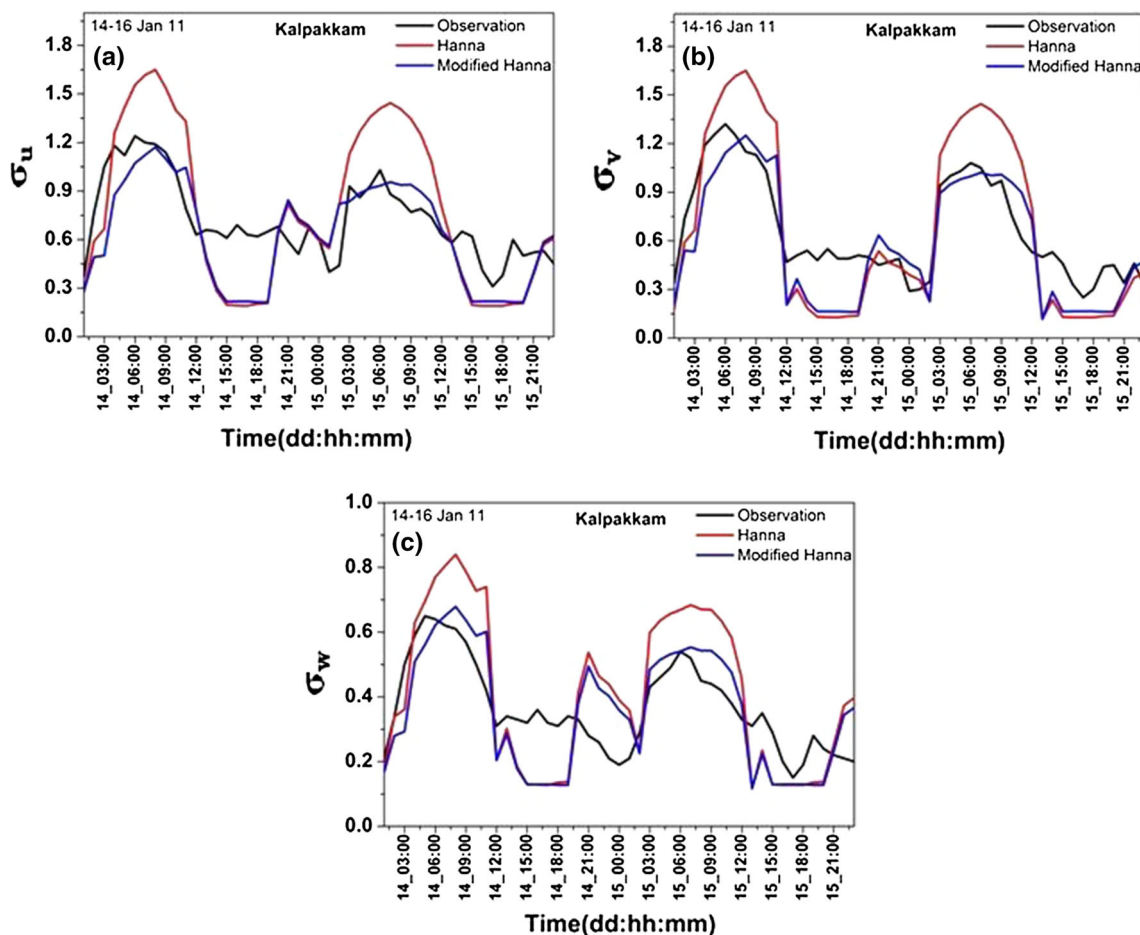
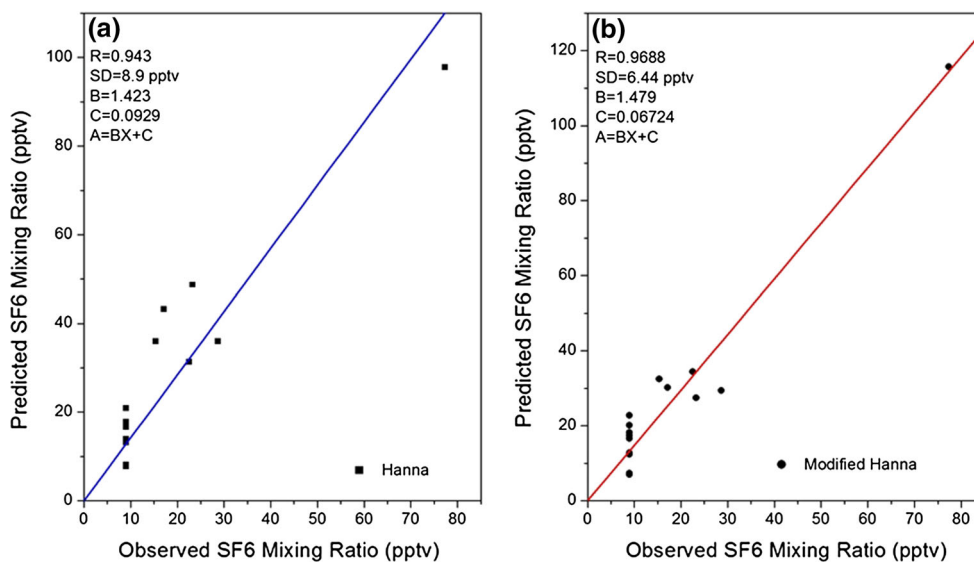


Fig. 7 Comparison of model derived turbulent intensities with default Hanna and modified Hanna relations along with observational estimates **a** σ_u , **b** σ_v , **c** σ_w for the winter case during 14–16 Jan 11 at Kalpakkam station

Fig. 8 FLEXPART predicted versus observed SF₆ mixing ratio using Hanna and modified Hanna diffusion relations for the dispersion experiment on 12/04/2013



and higher correlation. The study demonstrates that the Hanna turbulent diffusion relations are not universal for all the sites and for all the seasonal conditions and that it is

required to generate site- and season-specific, stability-dependent turbulent intensity relations for diffusion parameterization and dispersion assessment. The above

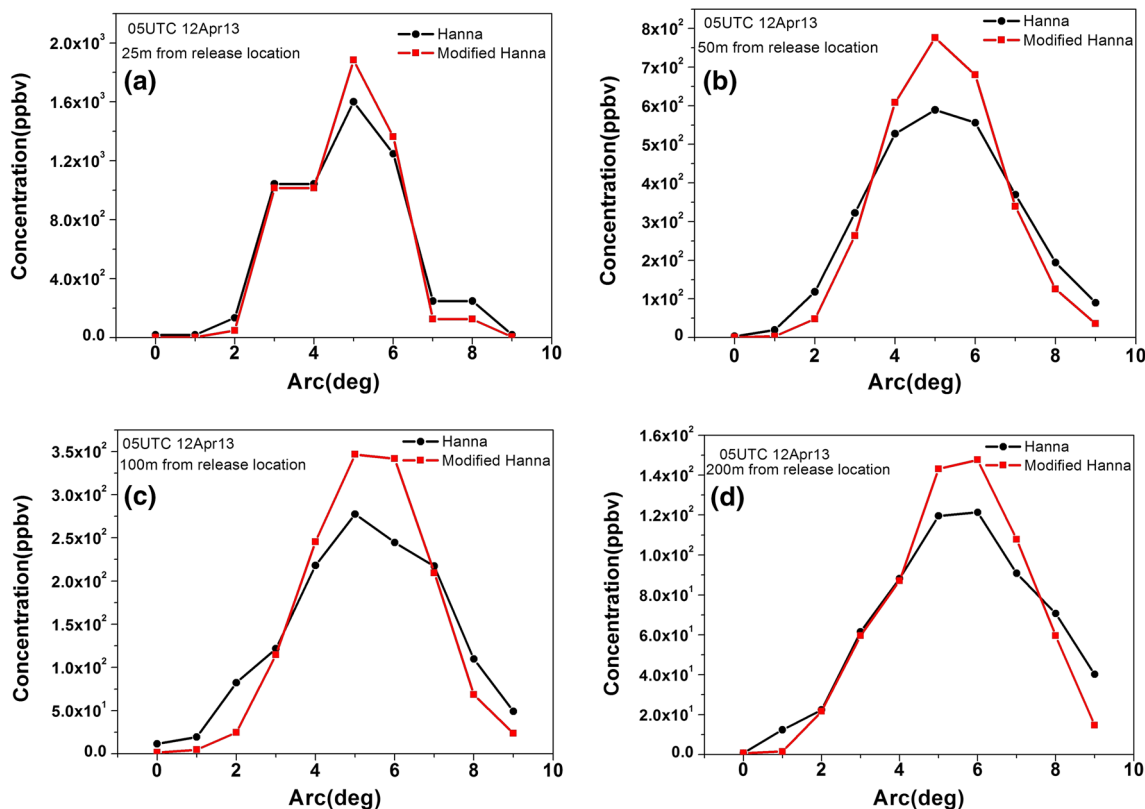


Fig. 9 Variation of simulated air concentration/mixing ratio (ppbv) at different downwind distances across the plume at arc distances of **a** 25 m, **b** 50 m, **c** 100 m, **d** 200 m from source point under unstable atmospheric condition during tracer experiment

Table 2 Statistical error metrics for the observed versus predicted concentrations with the two diffusion schemes for the Tracer Experiment at Kalpakkam site on 12 April 2013

Diffusion scheme	RMSE	FB	R	FS
Hanna scheme	13.32	-0.47	0.943	-0.41
Modified Hanna scheme	13.06	-0.42	0.969	-0.22

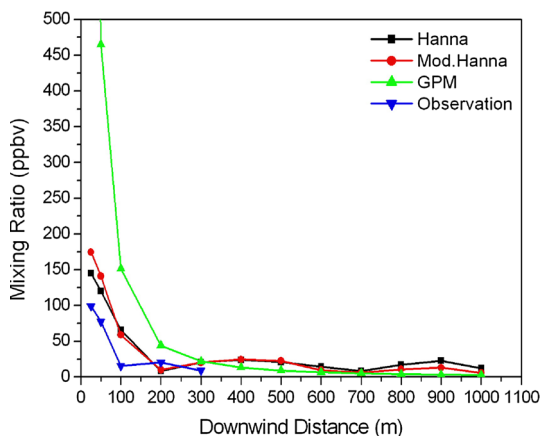


Fig. 10 Simulated plume centerline concentration/mixing ratio (ppbv) of SF₆ using Hanna and modified schemes of FLEXPART and Gaussian Plume model along with measured concentrations during the tracer experiment on 12 April 2013

results clearly demonstrate that the derived turbulent intensity relationships provide better agreement of concentrations with experimental data sets collected at the tropical coastal site Kalpakkam in India in terms of better cross-wind horizontal plume dispersion relative to the default Hanna scheme. The new relationships find potential application for assessing the industrial plume concentration or radioactive dose estimates for environmental impact under various prevailing weather conditions at the Kalpakkam site.

Acknowledgments Authors thank Sri S. A. V. Satya Murty, Director, EIRSG for the encouragement in carrying out the study. The observations used in the study were obtained from the Round Robin Exercise (RRE) project coordinated by IGCAR and funded by Board of Research in Nuclear Sciences, DAE, Mumbai. ARW model was obtained from NCAR, USA. Authors sincerely thank Dr. Jeromoe Fast for providing the Flexpart-WRF code. The authors thank the reviewers for their technical comments and suggestions which helped to improve the quality of the manuscript.

References

Beljaars ACM, Betts AK (1993) Validation of the boundary layer representation in the ECMWF model. In: Proceedings, ECMWF

- Seminar on Validation of Models over Europe, vol II. European Centre for Medium-Range Weather Forecasts, Shinfield Park, UK, pp 159–195, 7–11 September 1992
- Businger JA, Wyngaard JC, Izumi I, Bradley E (1971) Flux–profile relationships in the atmospheric surface layer. *J Atmos Sci* 28:181–189
- Carvalho JD, Degrazia GA, Anfossi D, De Campos CRJ, Roberti DR, Kerr AS (2002) Lagrangian stochastic dispersion modelling for the simulation of the release of contaminants from tall and low sources. *Meteorol Z* 11:89–97
- Deardorff JW (1973) Three-dimensional numerical modeling of the planetary boundary layer. In: Haugen DA (ed) Workshop on micrometeorology. American Meteorological Society, Boston, pp 271–311
- Doran JC, Fast JD, Barnard JC, Laskin A, Desyaterik Y, Gilles MK, Hopkins RJ (2008) Applications of Lagrangian dispersion modeling to the analysis of changes in the specific absorption of elemental carbon. *Atmos Chem Phys* 8:1377–1389
- Draxler RR (1992) Hybrid single-particle Lagrangian integrated trajectories (HY-SPLIT): Version 3.0—User’s guide and model description. NOAA Tech Memo ERL ARL-195, p 26 and Appendices. National Technical Information Service, 5285 Port Royal Road, Springfield, VA 22161
- Dyer AJ (1974) A review of flux–profile relationships. *Bound Layer Meteorol* 7:363–372
- Fast JD, Easter RC (2006) A Lagrangian particle dispersion model compatible with WRF. In: 7th WRF Users’ Workshop, NCAR, June 19–22. Boulder, CO, p 6.2
- Golder D (1972) Relations among stability parameters in the surface layer. *Bound Layer Meteorol* 3:47–58
- Hanna SR (1968) A method of estimating vertical eddy transport in the planetary boundary layer using characteristics of the vertical velocity spectrum. *J Atmos Sci* 25:1026–1033
- Hanna SR (1982) Applications in Air Pollution Modelling. In: Nieuwstadt FTM, Van Dop H (eds) Atmospheric Turbulence and Air Pollution Modeling. Reidel Publishing Co., Dordrecht, Holland, pp 275–310
- Hanna SR (1989) Confidence limits for air quality model evaluations, as estimated by bootstrap and jackknife resampling methods. *Atmos Environ* 23:1385–1398
- Hari Prasad KBRR, Srinivas CV, Bagavath Singh A, Vijaya Bhaskara Rao S, Baskaran R, Venkatraman B (2014) Numerical simulation and intercomparison of boundary layer structure with different PBL schemes in WRF using experimental observations at a tropical site. *Atmos Res* 145:27–44
- Holmes NS, Morawska L (2006) A review of dispersion modelling and its application to the dispersion of particles: an overview of different dispersion models available. *Atmos Environ* 40(30):5902–5928
- Holtslag AAM, Boville BA (1993) Local versus nonlocal boundary-layer diffusion in a global climate model. *J Clim* 6:1825–1842. doi:10.1175/1520-0442(1993)006<1825:LVNBLD>2.0.CO
- Hong SY, Noh Y, Dudhia J (2006) A new vertical diffusion package with an explicit treatment of entrainment processes. *Mon Weather Rev* 134:2318–2341
- Imai K, Chino M, Ishikawa H, Kai M, Asai K, Homma T, Hidaka A, Nakamura Y, Iijima T, Morichi S (1985) SPEEDI: a computer code system for the real-time prediction of radiation dose to the public due to an accidental release. Japan Atomic Research Institute Report JAERI p 1297. 87
- Irwin JS (1979) Estimating plume dispersion, a recommended generalized scheme. U.S. Environmental Protection Agency, Washington, DC, EPA/600/J-79/022 (NTIS PB299405)
- Jimenez PA, Dudhia J (2012) Improving the representation of resolved and unresolved topographic effects on surface wind in the WRF Model. *J Appl Meteorol Climatol* 51:300–3016
- Kaimal JC, Wyngaard JC, Izumi Y, Coté OR (1972) Spectral characteristics of surface layer turbulence. *Q J R Meteorol Soc* 98:563–589
- Kaimal JC, Wyngaard JC, Haugen DA, Cote OR, Izumi Y, Caughey SJ, Readings CJ (1976) Turbulence structure in the convective boundary layer. *J Atmos Sci* 33:2152–2169
- Kaimal JC, Eversole RA, Lenschow DH, Stankov BB, Kahn PH, Businger JA (1982) Spectral characteristics of the convective boundary layer over uneven terrain. *J Atmos Sci* 39:1098–1114
- Kantha LH, Clayson CA (2000) Small scale processes in geophysical fluid flows, 67., International Geophysics Series Academic Press, San Diego 883
- Karmen B, Zvezdana BK, Željko V (2012) Determining a turbulence averaging time scale by Fourier analysis for the nocturnal boundary layer. *GEOFIZ* 29(1):35–51
- Legg BJ, Raupach MR (1982) Markov-Chain simulation of particle dispersion in homogenous flows: the mean drift velocity induced by gradient in Eulerian velocity variance. *Bound Layer Meteorol* 24:3–13
- McBean GA (1971) The variations of the statistics of wind, temperature and humidity fluctuations with stability. *Bound Layer Meteorol* 1:438–457
- McNider RT, Moran MD, Pielke RA (1998) Influence of diurnal and internal boundary layer oscillations on large scale dispersion. *Atmos Environ* 22:2445–2462
- Metzger M, Holmes H (2008) Time scales in the unstable atmospheric surface layer. *Bound Layer Meteorol* 126:29–50
- Moreira VS, Degrazia GA, Roberti DR, Timm AU, Carvalho JC (2011) Employing a Lagrangian stochastic dispersion model and classical diffusion experiments to evaluate two turbulence parameterization schemes. *Atmos Pollut Res* 2(3):384–393
- Oncley SP, Friehe CA, Businger JA, Itsweire EC, LaRue JC, Chang SS (1996) Surface layer fluxes, profiles and turbulence measurements over uniform terrain under near-neutral conditions. *J Atmos Sci* 53:1029–1044
- Panofsky HA, Tennekes H, Lenschow DH, Wyngaard JC (1977) The characteristics of turbulent velocity components in the surface layer under convective conditions. *Bound Layer Meteorol* 11:355–361
- Seaman NL (2000) Meteorological modeling for air-quality assessments. *Atmos Environ* 34:2231–2259
- Singha A, Sadr R (2012) Characteristics of surface layer turbulence in coastal area of Qatar. *Environ Fluid Mech* 12:515–531
- Smagorinsky J (1963) General circulation experiments with the primitive equations: 1. The basic experiment. *Mon Weather Rev* 91:99–164
- Srinivas CV, Bagavath Singh A, Venkatesan R, Baskaran R (2011) Creation of benchmark meteorological observations for RRE on atmospheric flowfield simulation at Kalpakkam. IGC Report—213. Indira Gandhi Centre for Atomic Research, Kalpakkam 603102, Tamilnadu, India
- Srinivas CV, Venkatesan R, Baskaran R, Rajagopal V, Venkatraman B (2012) Regional scale atmospheric dispersion simulation of accidental releases of radionuclides from Fukushima Dai-ichi reactor. *Atmos Environ* 61:66–84
- Srinivas CV, Rakesh PT, Hari Prasad KBRR, Venkatesan R, Baskaran R, Venkatraman B (2014) Assessment of atmospheric dispersion and radiological impact from the Fukushima accident in a 40-km range using a simulation approach. *Air Qual Atmos Health* 7:209–227
- Stohl A, Thomson DJ (1999) A density correction for Lagrangian Particle dispersion model. *Bound Layer Meteorol* 90:155–167
- Stohl A, Forster C, Frank A, Seibert P, Wotawa G (2005) Technical note: the Lagrangian particle dispersion model FLEXPART version 6.2. *Atmos Chem Phys Disc* 5:4739–4799
- Stull RB (1988) An introduction to boundary layer meteorology. Kluwer, Dordrecht, Holland, p 680

- Srinivas CV, Bagavath Singh A, Surya Prakash G, Gopalakrishnan V, Rakesh PT, Sailesh Joshi, Venkatesan R, Subramanian V, Sivasubramanian K, Baskaran R, Venkatraman B (2013) Atmospheric Dispersion Experiments using SF₆ tracer during summer condition in April 2013 at Kalpakkam coastal site. Report IGC/SG/RSD/RIAS/92617/GN/3014/REV-A, Radiological Safety Division, Indira Gandhi Centre for Atomic Research, Kalpakkam, p 31
- Thomson DJ (1987) Criteria for the selection of stochastic models of particle trajectories in turbulent flows. *J Fluid Mech* 180:529–556
- Troen I, Mahrt L (1986) A simple model of the atmospheric boundary layer: sensitivity to surface evaporation. *Bound Layer Meteorol* 37:129–148
- Vecenaj Z, De Wekker SFJ, Grubisic V (2011) Near-surface characteristics of the turbulence structure during a mountain-wave event. *J Appl Meteorol Climatol* 50:1088–1106
- Vecenaj Z, Belusic D, Grubisic V, Grisogono B (2012) A long-coast features of bora-related turbulence. *Bound Layer Meteorol* 143:527–545
- Vickers D, Mahrt L (1996) Quality control and flux sampling problems for tower and aircraft data. *J Atmos Ocean Technol* 14:512–526
- Willis GE, Deardorff JW (1981) A Laboratory study of dispersion in the middle of the convectively mixed layer. *Atmos Environ* 15:109–117
- Wilson JD, Sawford BL (1996) Review of lagrangian stochastic models for trajectories in the turbulent atmosphere. *Bound Layer Meteorol* 78:191–210
- Wilcjack JM, Oncley SP, Stage SA (2001) Sonic anemometers tilt corrections algorithms. *Bound Layer Meteorol* 99:127–150
- Zannetti P (1990) Air pollution modelling: theories, computational methods and available software. Computational Mechanics Publications, Southampton Boston, p 444 (Van Nostrand Reinhold, New York)
- Zannetti P (1992) Particle modeling and its application for simulating air pollution phenomena. In: Melli P, Zannetti P (eds) *Environmental Modelling*. Computational Mechanics Publications, Southampton